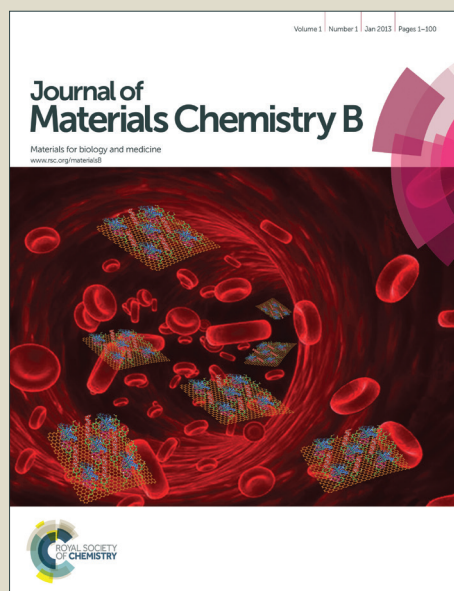


Journal of Materials Chemistry B

Accepted Manuscript



This is an *Accepted Manuscript*, which has been through the Royal Society of Chemistry peer review process and has been accepted for publication.

Accepted Manuscripts are published online shortly after acceptance, before technical editing, formatting and proof reading. Using this free service, authors can make their results available to the community, in citable form, before we publish the edited article. We will replace this *Accepted Manuscript* with the edited and formatted *Advance Article* as soon as it is available.

You can find more information about *Accepted Manuscripts* in the [Information for Authors](#).

Please note that technical editing may introduce minor changes to the text and/or graphics, which may alter content. The journal's standard [Terms & Conditions](#) and the [Ethical guidelines](#) still apply. In no event shall the Royal Society of Chemistry be held responsible for any errors or omissions in this *Accepted Manuscript* or any consequences arising from the use of any information it contains.

Cite this: DOI: 10.1039/c0xx00000x

www.rsc.org/xxxxxx

Communication

Temperature-triggered shape-transformations in layer-by-layer microtubes

Choonghyun Sung, Ajay Vidyasagar, Katelin Hearn, and Jodie L. Lutkenhaus*

Received (in XXX, XXX) Xth XXXXXXXXX 20XX, Accepted Xth XXXXXXXXX 20XX

DOI: 10.1039/b000000x

One-dimensional layer-by-layer (LbL) nano- and microtubes have been extensively studied for energy and biomedical applications. Here, we report a temperature-triggered transformation in shape for LbL microtubes consisting of poly(allylamine hydrochloride) (PAH) and poly(acrylic acid) (PAA). PAH/PAA microtubes were assembled onto porous sacrificial templates. Released microtubes transform to closed ellipsoids upon heating in water. On the other hand, unreleased microtubes (remaining within the template) exhibit a completely different behavior in which periodic perforations appear, suggestive of Rayleigh instabilities. In both cases, the transformations occurred near and above the glass transition temperature (T_g) of the hydrated PAH/PAA LbL assembly, suggesting that the transformation in shape is tied to the thermal properties of the LbL assembly.

LbL assembly is a versatile technique used to build functional thin films and nanostructures for applications ranging from energy to health.¹⁻³ Oppositely charged polyelectrolytes are alternately adsorbed onto various substrates with rinsing steps in between. An LbL assembly's growth, structure, and properties can be fine-tuned using polymer chemistry and assembly conditions such as pH and salt concentration.^{4, 5} Besides polyelectrolytes, other materials such as inorganic and metallic nanoparticles as well as biomacromolecules may act as the adsorbing species.^{2, 6}

LbL microcapsules and microtubes have emerged as promising materials for drug delivery.⁷⁻¹⁰ Using sacrificial spherical particles or porous templates, an LbL assembly is deposited, resulting in microcapsules or microtubes, respectively, following template dissolution.¹¹ Hollow LbL microcapsules consisting of poly(diallyldimethyl-ammonium chloride) (PDAC) and poly(styrene sulfonate) (PSS) have exhibited a characteristic response upon heating – either shrinking or swelling, depending upon the outermost layer and the balance of hydrophobic and electrostatic forces.¹²⁻¹⁵ Elsewhere, PAH/PSS LbL microcapsules have exhibited shrinkage upon heating.¹⁶⁻¹⁹ This behavior was tied to a “glass-melt” transition.^{13, 14}

We recently identified this transition using quartz crystal microbalance with dissipation (QCM-D), in which it was demonstrated that the transition is accompanied by a large flux of water into or out of the LbL assembly depending on whether it shrinks or swells.^{20, 21} The transition itself exhibits many features

typical of a glass transition temperature (T_g), (sigmoidal heat capacity, dramatic changes in mechanical properties and diffusion). We have also found that LbL assemblies containing weak polyelectrolytes PAH and PAA undergo a glass transition in water for most assembly pH values with the exception when both polyelectrolytes are fully charged. It should be noted that this transition has been called a “glass transition” or a “glass-melt transition”, but the underlying process is likely very different from a traditional glass transition because ion pairs and water are involved.

Considering that hollow LbL capsules have shown dramatic changes in size in response to temperature, we hypothesized that LbL microtubes would exhibit an analogous unique response. Hollow LbL capsules retain their spherical shape during the transition, but LbL microtubes may not. Early work by He *et al.* showed that PAH/PSS microtubes transform to spheres and hollow capsules upon high-temperature incubation, although only a limited temperature range and only free microtubes were explored.²²

Here, we investigated the temperature-triggered shape transformation of released and unreleased PAH/PAA LbL microtubes in water as a function of temperature and time. The PAH/PAA LbL system is of particular interest because it offers future opportunities as a pH-responsive material. The temperature-response of unreleased LbL microtubes (in which the tubes remain in the template) is of interest because the substrate/film interface plays an additional role. Drastically different transformations are observed for the two scenarios. Results are discussed in the context of LbL film structure, properties, and surface interactions. To our knowledge, this is the first investigation of temperature-triggered changes in shape for LbL microtubes consisting solely of weak polyelectrolytes.

To study the transformation of LbL microtubes in water, two different experimental routes were employed, Fig. 1. In Route A, a PAH/PAA LbL film is deposited onto an ion track-etched polycarbonate template. Film deposited on the template's surface is removed, the membrane is dissolved, and the released microtubes are purified via dialysis. The microtubes are then incubated at the time and temperature of interest, and dried for further analysis. In Route B, the LbL-coated membrane is incubated in water at the desired temperature. The microtubes are then released from the membrane for further analysis. The main difference between the two routes is whether microtubes are incubated when freely suspended (Route A) or when bound to the

membrane pore (Route B).

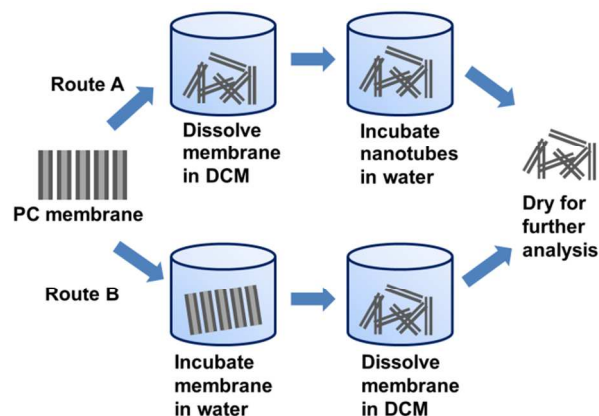


Fig.1 A schematic illustration of the two Routes. In Route A, microtubes are released from the membrane and then incubated. In Route B, the unreleased microtubes are incubated and then released.

Route A. Incubation of released LbL microtubes. Fig. 2 shows images of microtubes prior to high temperature incubation. Fig. 2a and b show typical scanning electron microscopy (SEM) and transmission electron microscopy (TEM) images of (PAH/PAA)₁₀ microtubes released from the template using dichloromethane (DCM). (The subscript in (PAH/PAA)₁₀ is indicative of the number of layer pairs deposited). The microtubes' length (10 μm) and diameter (1 μm) were comparable to the original dimensions of the template's pores. The tubular structure is clearly present in the TEM image shown in Fig. 2b, from which the average wall thickness was estimated to be 110 nm. Following dialysis in water to remove residual DCM, the microtubes appear to soften and contract to 5.1 μm in length and 1 μm in diameter, Fig. 2c. Confocal laser scanning microscopy (CLSM) of the dialyzed microtubes in water also shows the microtubes' contraction and wall-thickening to 390 nm, Fig. 2d and Fig. S1a, ESI†. Many of the microtubes appear to retain their hollow shape.

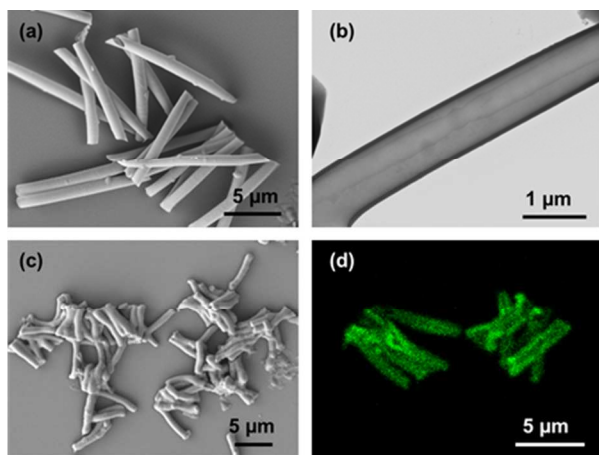


Fig. 2 (a) SEM and (b) TEM images of microtubes released from the sacrificial membrane using dichloromethane. (c) SEM image of the microtubes after dialysis in water. (d) CLSM image of microtubes in water at room temperature.

The effect of high temperature incubation on the transformation of the LbL microtubes in water was investigated for varying incubation temperatures ranging from room temperature to 121 °C, Fig. 3. At all incubation temperatures, except 121 °C, the incubation time was 1 hour. At 121 °C, the incubation temperature was 45 min. Generally, as the incubation temperature increased, the microtubes contracted and the outer diameter increased. LbL microtubes incubated at 85 and 95 °C did not exhibit a hollow tubular structure as confirmed using TEM (Fig. S1b and c, ESI†), and the majority of the incubated microtubes appear to have closed ends. At 121 °C, fairly spherical/ellipsoid shapes are observed as shown in Fig. 3c and d. These results suggest that this transition from open to closed structures might be applicable for the encapsulation of small molecules. The transformation is irreversible; even after 1 week the ellipsoid shapes remained intact.

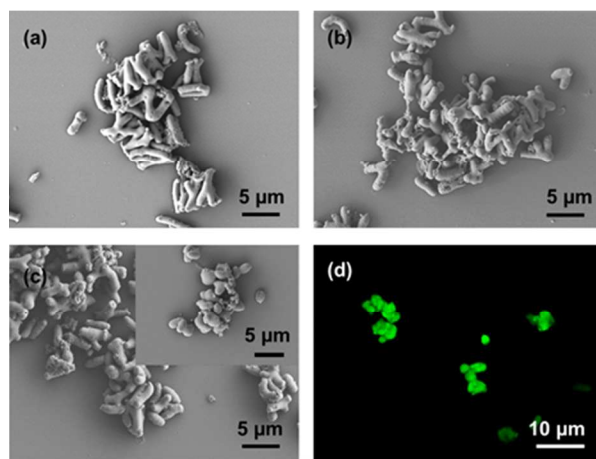


Fig. 3 SEM images of the microtubes incubated at (a) 70, (b) 95, and (c) 121 °C. CLSM image of the microtubes in water after incubated at 121 °C.

To study the effect of incubation time, microtube suspensions were incubated for varying times at a fixed temperature, 70°C, Fig. S2, ESI†. Generally, the microtubes shorten and fatten as incubation proceeds. After 5 hr, the shape became similar to that of the samples incubated at 121 °C for 45 min. This demonstrates that incubation time can be used to control the transformation at low incubation temperatures. However at 121 °C, the transformation rapidly proceeded within the first 15 min.

To quantify the effect of the incubation temperature and time, the length and outer diameter of microtubes were measured from multiple SEM images. Fig. 4a shows the effect of incubation temperature on the microtube dimensions. As the incubation temperature increased, the microtubes' length decreased and diameter increased. Above 85 °C, the length remained fairly constant. However, the microtubes' outer diameter increased linearly as the incubation temperature increased. It should be noted that some microtubes incubated at temperatures greater than 95 °C merged to form larger structures (evident in Fig. 3c and d), resulting in increased error for the outer diameter. Fig. 4b shows the effect of incubation time on the microtube dimensions at a fixed incubation temperature of 70 °C. The microtubes' length decreased rapidly in the first hour and leveled off after 2 hr of incubation. The microtubes' outer diameter also increased with incubation time.

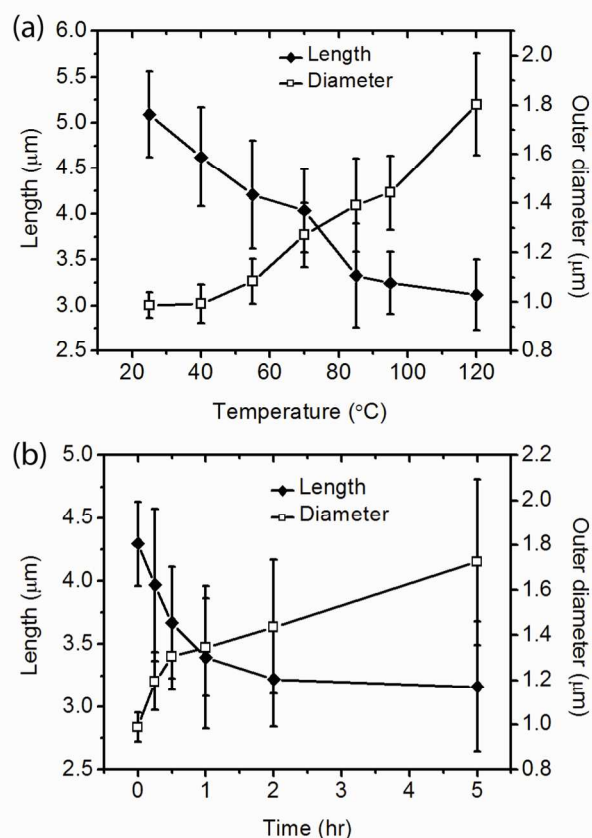


Fig. 4 Length and outer diameter of (PAH/PAA)₁₀ microtubes as a function of (a) incubation temperature (incubation time as noted in main text) and (b) incubation time at 70 °C.

The temperature-triggered transformation of microtubes did not depend on the microtubes' innermost layer. For instance, (PAH/PAA)₁₀PAH microtubes showed similar results to (PAH/PAA)₁₀ (Fig. S3 and S4, ESI†). This result is in contrast to the known odd-even effect for PDAC/PSS LbL microcapsules discussed previously. The lack of odd-even effect for PAH/PAA LbL microtubes suggests that hydrophobic forces dominate upon incubation, in which the PAH/PAA microtube contracts regardless of the identity of the inner layer. The aspect ratio of the microtubes decreases from about 5 to about 1.7 as incubation temperature increases from room temperature to 121 °C. The reduction in aspect ratio further supports the idea that hydrophobic forces dominate, in which a reduction in water/tube contact area occurs upon incubation. At extended times and temperatures, the tubes merged with each other, further reducing the contact area and increasing the apparent volume (Fig. S5, ESI†).

Route B. Incubation of unreleased LbL microtubes. After depositing LbL assemblies onto porous templates, the LbL-coated templates were incubated at varying temperatures in water. Then, the incubated membranes were selectively dissolved in DCM to release the resulting microtubes, Fig. 5. As the incubation temperature increased, perforations appeared at a fairly regular spacing, whereas the microtubes' length remained unchanged. Above 70 °C the number of perforations greatly increased, whereas at lower incubation temperatures they were observed infrequently. The center-to-center spacing between the

perforations was $3.5 \pm 0.8 \mu\text{m}$, and the perforation's diameter was $1.5 \pm 0.3 \mu\text{m}$ for microtubes incubated at 70 °C. From the pronounced darkening in the microtubes' wall (Fig. 6d vs. Fig. 2b) it appears that the microtube wall thickens as the perforations form. Of note, the temperature at which the perforations regularly appear coincides with the T_g ($71 \pm 7 \text{ °C}$) as measured using modulated differential scanning calorimetry (Fig. S6 and Table S1, ESI†).

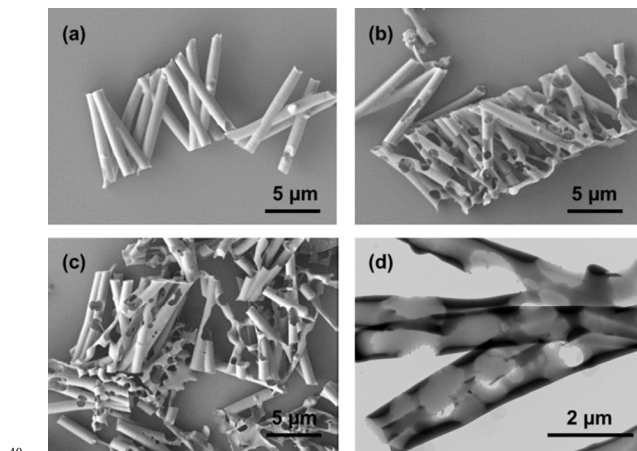


Fig. 5 SEM images of microtubes that had been incubated in water at temperatures of (a) 40, (b) 55, (c) 85 °C during which the microtubes were confined to the template. (d) TEM image of microtubes incubated at 85 °C. Microtubes were released and dried from DCM.

The regularity and periodicity of the observed perforations is suggestive of Rayleigh instabilities. When the free surface of a liquid cylinder undulates with a wavelength larger than the perimeter of the cylinder, the liquid cylinder responds by decreasing the surface area and the amplitude of undulation grows. Eventually, the liquid cylinder disintegrates into droplets.²³ For a thin liquid film inside a capillary of radius R , the wavelength (spacing between voids) is $\lambda = 8.89R$.²⁴ For our 1 μm diameter microtubes, the characteristic wavelength is 4.4 μm, whereas our actual spacing is $3.5 \pm 0.8 \mu\text{m}$. The two values show good agreement, and any minor discrepancy might arise from electrostatic interactions²² or the finite wall thickness of the microtube.²⁵ Our results compare well to Rayleigh instabilities observed for nanotubes of poly(methylmethacrylate) (PMMA), polystyrene (PS), PMMA/PS blends, and poly(styrene-*b*-2-vinylpyridine), in which periodic holes were observed upon thermal annealing.²⁵⁻³¹

It is curious that we should observe drastically different transitions in shape for released and unreleased LbL microtubes. The materials and assembly are identical, as are the incubation conditions. The remaining factor, then, is the interaction between the templates' pore wall and the LbL assembly. Rayleigh instabilities are driven by surface energy; therefore, microtubes produced by the two Routes should have very different surface energies. In the case of Route A, microtubes are fully surrounded by water during incubation. The cylinder-to-sphere transition shares similarities to the predictions of Nichols et al. in which a critical length-to-diameter ratio of 7.2 was derived.³² Below this critical ratio, a single tube transforms into a single sphere; above the ratio, multiple particles are formed. In our case the length-to-diameter ratio is 10, which is only slightly above the critical ratio.

Thus, it is possible that the microtubes formed via Route A desire to form Rayleigh instabilities upon incubation, but are too short to do so.

In the case of unreleased microtubes prepared from Route B, there exist attractive interactions between the pore wall and the layer-by-layer assembly. These interactions possibly pin the microtube's outer wall to the pore wall, thus drastically changing the surface energy. Upon incubation, the LbL microtube desires to contract, but its interaction with the wall prevents it from doing so. Instead, to minimize the surface energy, Rayleigh instabilities form during the incubation process for the unreleased microtubes.

He et al. reported the transformation of PAH/PSS LbL microtubes to microcapsules, when microtube suspensions were incubated at 121 °C for 20 min.²² This system consists of a weak polyelectrolyte and a strong polyelectrolyte. Rayleigh instabilities were suggested as a possible mechanism. In light of the discussion above and the results found herein, Rayleigh instabilities are indeed a possible cause. The change in wall thickness was not reported and only a limited range of temperature and time was explored, so further work is required to fully understand the PAH/PSS system.

There remains a question as to whether mass is conserved for the PAH/PAA microtube over the course of the transition. PDAC/PSS microcapsules exhibited mass loss during incubation, but it is not known if PAH/PAA microtubes behave similarly. Our prior work with QCM-D of PAH/PAA LbL films indicates that mass changes slightly at the thermal transition, but this was associated with flux of water into and out of the film rather than loss of polyelectrolyte.²¹

Because the PAH/PAA LbL microtubes consists solely of weak polyelectrolytes, we expect that they should exhibit pronounced changes in shape in response to pH. For instance, LbL microtubes arrays have exhibited pronounced swelling in response to pH.³³ The dual pH/temperature-response of our microtubes will be a subject of further exploration.

Conclusion

The temperature-triggered transformation of released and unreleased PAH/PAA microtubes in water was studied. Released microtubes contract into spheres and ellipsoids and unreleased microtubes exhibit Rayleigh instabilities upon incubation. In both cases, the transformation occurred near the T_g for hydrated PAH/PAA LbL assemblies. These results suggest that the surrounding media, whether it is water or a solid pore wall, can have a strong influence on the temperature-response of an LbL microtube. This temperature-triggered transformation has potential applications for the encapsulation of drugs, small molecules, and separations. Because this system is comprised of weak polyelectrolytes, it also bears the possibility of dual pH/temperature-responsive behavior.

Notes and references

^a Artie McFerrin Department of Chemical Engineering, Texas A&M University, College Station, Texas 77843, USA.

^a Artie McFerrin Department of Chemical Engineering, Texas A&M University, College Station, Texas 77843, USA. Email :

jodie.lutkenhaus@tamu.edu

Acknowledgements

This material is based upon work supported by the National Science Foundation under Grant No. 1049706.

1. G. Decher, *Science*, 1997, 277, 1232-1237.
2. A. P. R. Johnston, C. Cortez, A. S. Angelatos and F. Caruso, *Curr. Opin. Colloid Interface Sci.*, 2006, 11, 203-209.
3. O. Azzaroni and K. H. A. Lau, *Soft Matter*, 2011, 7, 8709-8724.
4. R. von Klitzing, *Physical Chemistry Chemical Physics*, 2006, 8, 5012-5033.
5. P. Lavalle, J. C. Voegel, D. Vautier, B. Senger, P. Schaaf and V. Ball, *Advanced Materials*, 2011, 23, 1191-1221.
6. L. L. del Mercato, P. Rivera-Gil, A. Z. Abbasi, M. Ochs, C. Ganas, I. Zins, C. Sonnichsen and W. J. Parak, *Nanoscale*, 2010, 2, 458-467.
7. K. Kohler and G. B. Sukhorukov, *Advanced Functional Materials*, 2007, 17, 2053-2061.
8. W. J. Tong, S. P. She, L. L. Xie and C. Y. Gao, *Soft Matter*, 2011, 7, 8258-8265.
9. A. L. Becker, A. P. R. Johnston and F. Caruso, *Small*, 2010, 6, 1836-1852.
10. T. Komatsu, *Nanoscale*, 2012, 4, 1910-1918.
11. Y. Wang, A. S. Angelatos and F. Caruso, *Chemistry of Materials*, 2008, 20, 848-858.
12. C. Y. Gao, S. Leporatti, S. Moya, E. Donath and H. Mohwald, *Chemistry-a European Journal*, 2003, 9, 915-920.
13. K. Kohler, D. G. Shchukin, H. Mohwald and G. B. Sukhorukov, *Journal of Physical Chemistry B*, 2005, 109, 18250-18259.
14. K. Koehler, H. Moehwald and G. B. Sukhorukov, *Journal of Physical Chemistry B*, 2006, 110, 24002-24010.
15. C. Dejuguat, K. Kohler, M. Dubois, G. B. Sukhorukov, H. Mohwald, T. Zemb and P. Guttman, *Advanced Materials*, 2007, 19, 1331-+.
16. K. Kohler, D. G. Shchukin, G. B. Sukhorukov and H. Mohwald, *Macromolecules*, 2004, 37, 9546-9550.
17. S. Leporatti, C. Gao, A. Voigt, E. Donath and H. Mohwald, *European Physical Journal E*, 2001, 5, 13-20.
18. A. V. Dubrovskii, L. I. Shabarchina, Y. A. Kim and B. I. Sukhorukov, *Russian Journal of Physical Chemistry*, 2006, 80, 1703-1707.
19. G. Ibarz, L. Dahne, E. Donath and H. Mohwald, *Chemistry of Materials*, 2002, 14, 4059-4062.
20. A. Vidyasagar, C. Sung, R. Gamble and J. L. Lutkenhaus, *ACS Nano*, 2012, 6, 6174-6184.
21. A. Vidyasagar, C. Sung, K. Losensky and J. L. Lutkenhaus, *Macromolecules*, 2012, 45, 9169-9176.
22. Q. He, W. Song, H. Moehwald and J. Li, *Langmuir*, 2008, 24, 5508-5513.
23. L. Rayleigh, *Proceedings of the London Mathematical Society*, 1878, s1-10, 4-13.
24. F. A. Nichols and W. W. Mullins, *Transactions of the Metallurgical Society of Aime*, 1965, 233, 1840-&.
25. J. T. Chen, M. F. Zhang and T. P. Russell, *Nano Letters*, 2007, 7, 183-187.
26. S. Schlitt, A. Greiner and J. H. Wendorff, *Macromolecules*, 2008, 41, 3228-3234.
27. X. D. Feng and Z. X. Jin, *Macromolecules*, 2009, 42, 569-572.
28. D. Chen, J. T. Chen, E. Glogowski, T. Emrick and T. P. Russell, *Macromolecular Rapid Communications*, 2009, 30, 377-383.
29. X. D. Feng, S. L. Mei and Z. X. Jin, *Langmuir*, 2011, 27, 14240-14247.
30. S. L. Mei, X. D. Feng and Z. X. Jin, *Macromolecules*, 2011, 44, 1615-1620.
31. P.-W. Fan, W.-L. Chen, T.-H. Lee and J.-T. Chen, *Macromolecular Rapid Communications*, 2012, 33, 343-349.
32. F. A. Nichols, *J. Mater. Sci.*, 1976, 11, 1077-1082.
33. K. K. Chia, M. F. Rubner and R. E. Cohen, *Langmuir*, 2009, 25, 14044-14052.

Freely released microtubes in water transform to ellipsoids and spheres at high temperatures, while microtubes bound to the template surface showed periodic voids suggestive of Rayleigh instabilities.

